Eur Biophys J (2007) 37:1–10
DOI 10.1007/s00249-007-0144-4

ORIGINAL PAPER

Structural transition temperature of hemoglobins correlates with species' body temperature

Kay Frank Thorsten Zerlin · Nicole Kasischke · Ilya Digel · Christina Maggakis-Kelemen · Aysegül Temiz Artmann · Dariusz Porst · Peter Kayser · Peter Linder · Gerhard Michael Artmann

Received: 20 September 2006 / Revised: 1 February 2007 / Accepted: 8 February 2007 / Published online: 28 March 2007

Abstract Human red blood cells (RBCs) exhibit sudden changes in their biophysical properties at body temperature (T_B). RBCs were seen to undergo a spontaneous transition from blockage to passage at $T_C = 36.4 \pm 0.3$°C, when the temperature dependency of RBC-passages through 1.3 μm narrow micropipettes was observed. Moreover, concentrated hemoglobin solutions (45 g/dl) showed a viscosity breakdown between 36 and 37°C. With human hemoglobin, a structural transition was observed at T_B as circular dichroism (CD) experiments revealed. This leads to the assumption that a species' body temperature occupies a unique position on the temperature scale and may even be imprinted in the structure of certain proteins. In this study, it was investigated whether hemoglobins of species with a T_B different from those of human show temperature transitions and whether those were also linked to the species' T_B. The main conclusion was drawn from dynamic light scattering (DLS) and CD experiments. It was observed that such structural temperature transitions did occur in hemoglobins from all studied species and were correlated linearly (slope 0.81, $r = 0.95$) with the species' body temperature. We presumed that α-helices of hemoglobin were able to unfold more readily around T_B. α-helical unfolding would initiate molecular aggregation causing RBC passage and viscosity breakdown as mentioned above. Thus, structural molecular changes of hemoglobin could determine biophysical effects visible on a macroscopic scale. It is hypothesized that the species' body temperature was imprinted into the structure of hemoglobins.

Keywords Protein dynamics · Hemoglobin · Structural transition · Denaturation

K. F. T. Zerlin · N. Kasischke · I. Digel · C. Maggakis-Kelemen · A. Temiz Artmann · D. Porst · P. Kayser · P. Linder · G. M. Artmann (✉)
Division Juelich, University of Applied Sciences Aachen, Ginsterweg 1, 52428 Juelich, Germany
e-mail: artmann@fh-aachen.de

Introduction

Micropipette aspiration experiments with human red blood cells (RBCs) (Artmann et al. 1998) were followed by viscometry studies with concentrated hemoglobin solutions (Kelemen et al. 2001). Arrhenius plots were obtained of Hb viscosimetry studies (Kelemen et al. 2001) suggesting first that the cellular phenomenon may be linked to hemoglobin. An obvious finding was the extremely high-activation energy (366.6 kJ/mol) within the temperature range of 35–38°C for concentrated hemoglobin solutions (50 g/dl) compared to 55.1–58.1 kJ/mol found for higher and lower temperatures, respectively. Such a non-linear behavior is in general, believed to be related to protein phase transitions (Glaser 2004). These micropipette aspirations experiments and viscosimetry studies showed macroscopic effects of cells and concentrated solutions. Subsequent circular dichroism (CD) measurements with diluted hemoglobin solutions (Artmann et al. 2004) were a first attempt to investigate a structural effects produced in hemoglobin molecules by temperature changes. The molecular studies (Artmann et al. 2004) underlined the idea of a correlation between biophysical properties of RBCs and the structural state of molecular hemoglobin.

Based on two-dimensional infrared spectroscopy, a two-step model of protein unfolding in human hemoglobin was proposed (Yan et al. 2003). An initial structural perturbation occurs between 30 and 44°C and is followed by initial

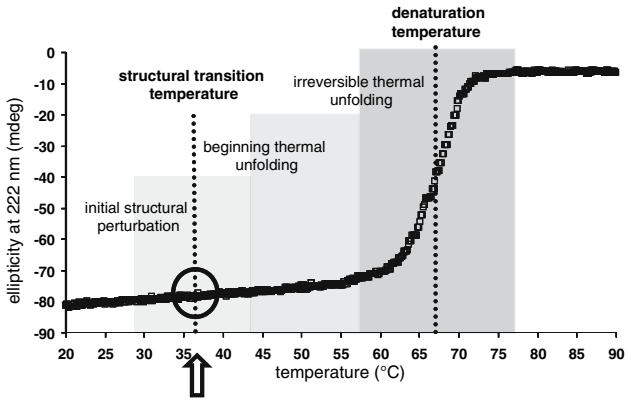

Fig. 1 Complete denaturation curve (*open squares*) of *Homo sapiens sapiens* hemoglobin obtained from CD temperature scans with a heating rate of 40°C/h. The ellipticity at 222 nm is presented in mdeg. The ''orbited'' area shows the region of the described (Yan et al. 2003) structural perturbation stage, the *gray* area represents the initial thermal unfolding stage and the *dark gray* area the stage of irreversible thermal unfolding of human Hb. The *black circle* marked with an *arrow* points at the structural transition temperature range in the perturbation stage near body temperature. The denaturation temperature of human Hb obtained from CD spectroscopy was 67.1°C

thermal protein unfolding between 44 and 54°C. The second step is irreversible and induces thermal aggregation between 54 and 70°C. Figure 1 shows an experimental denaturation curve of *Homo sapiens sapiens* hemoglobin (Hb) as obtained from CD data. The structural transition described in this paper occurred in the initial structural perturbation stage. In terms of ellipticity changes, this is only a 2.5% loss of total ellipticity between 30 and 40°C in contrast to the total denaturation. These small changes during the initial structural perturbation between 30 and 44°C are not visible on the scale in Fig. 1. Artmann et al. (2004) and Digel et al. (2006) observed under usage of CD spectroscopy human Hb and hemoglobins of monotremes and found there is especially this temperature interval (30–40°C) where significant structural changes are induced by slight temperature changes.

It may be assumed that there is a close relationship between critical temperatures of such structural transitions and a species' body temperature. First notes for this are results presented by Digel et al. (2006). It was shown that structural transitions temperatures of hemoglobin of monotremes are about 33.0°C likewise the species body temperature.

For this reason the hemoglobins of various animals with T_B different from those of humans (between 33 and 42°C) were analyzed. The species chosen are listed in the following with their corresponding T_B and common designation: *Tachyglossus aculeatus* (echidna, 33.0°C), *Ornithorhynchus anatinus* (platypus, 33.0°C), *Phascolarctos cinereus* (coala, 35.2°C), *Catagonus wagneri* (chacoan peccary, 36.17°C), *Homo sapiens sapiens* (human, 36.6°C), *Thylogale* sp. (dusty pademelon, 37.0°C), *Felis viverrina* (fishing cat, 37.6°C), *F. silvestris* forma *catus* (felis serval, 37.7°C), *Camelus bactrianus* (bactrian camel humphrey, 38.0°C), *Bos taurus taurus* (cow, 38.6°C), *Sus scrofa domestica* (pig, 39.7°C), *Gallus gallus domesticus* (chicken, 41.0°C), *Eurypyga helias* (greater sunbittern, 41.06°C), *Nucrifraga caryocatactes* (spotted nutcracker, 42.2°C) (Grigg et al. 2003; Penzlin 1977; Whittow 1971; J. Turnage, San Diego Zoological Society, San Diego, CA, USA, personal communication).

Experimental

Hemoglobin preparation

Hemoglobin was prepared from erythrocytes obtained from various animals. Approximately 1–2 ml of heparinized blood was obtained from each individual donor. RBCs were harvested by centrifugation at 500×*g* for 2 min. RBCs (0.5 ml) were washed in 9.5 ml buffer solution (0.1 M KCl, 61.3 mM K_2HPO_4 and 5.33 mM KH_2PO_4, pH 7.4 and 290 ± 10 mosm/kg, according to Cameron et al. 1988) three times at 500×*g* for 2 min and then hemolyzed in 3.6 ml distilled water. Ionic strength and pH of hemoglobin solutions were adjusted as close as possible to natural conditions in blood with this buffer used as described by Cameron et al. (1988).

Some experiments with *Homo sapiens sapiens*, *Sus scrofa domestica*, and *Bos taurus taurus* hemoglobin were carried out using lyophilized hemoglobin obtained from Sigma-Aldrich Chemie GmbH (Munich, Germany).

The hemolysates were diluted in the buffer solution and filtered twice through a 0.2–0.45 nm Whatman nitrocellulose filter to remove membrane pieces and dust particles. Hemoglobin prepared with this method is about 99% pure.

Concentrations were determined spectrophotometrically at 405 and 540 nm using a UV-Vis V-550 Jasco spectrophotometer (Jasco Labor- und Datentechnik GmbH, Groß-Umstadt, Germany) with a cell length of 1.0 cm (100-QS und 115B-QS, Firma Hellma GmbH & Co., KG, Müllheim, Germany). Spectrophotometric data were analyzed and interpreted according to Van Kampen and Zijlstra (1965) and Zwart et al. (1984).

Dynamic light scattering

Dynamic light scattering (DLS) measurements were carried out with a Dawn® EOS™ LS device connected with a Quasi elastic light scattering (QELS) module (both Wyatt Technology, Santa Barbara, CA, USA) using Astra 5.1 software for data acquisition and analysis. In experiments on dilute solutions, in which interactions between solute

molecules were taken to be negligible, it is usually sufficient to assume that a single solute species was present and that the measured mutual diffusion coefficient D of the solute was related to its hydrodynamic drag coefficient f by the Stokes–Einstein equation

$$D = \frac{K_b T}{f}, \quad (1)$$

where K_b is Boltzman's constant and T is the absolute temperature.

With these assumptions, the intensity–intensity correlation function of the scattered light is characterized by a single exponential with decay time Dk^2, k being the magnitude of the scattering vector k in the experiment. The normalized intensity autocorrelation function for detection arising from a single diffusive process with the decay constant Γ can be written as (Berne and Pecora 1976):

$$g^{(2)}(\tau) = \frac{G^{(2)}(\tau)}{\beta} = 1 + A e^{-\Gamma\tau} \quad (2)$$

with $\Gamma = DK^2$, where A is an instrument optical constant, D the diffusion coefficient and K is the magnitude of the scattering wave vector, defined as $(4\pi n/\lambda_0)$ sin $(\Theta/2)$ with n the refractive index of the medium, λ_0 the incident wavelength in vacuo and Θ the scattering angle. $G^{(2)}(\tau)$ is the unnormalized experimental autocorrelation function and the normalization constant β for $g^{(2)}(\tau)$ is chosen as

$$\beta = \lim_{\tau\to\infty} G^{(2)}(\tau). \quad (3)$$

Circular dichroism measurements

The far-UV CD spectra were measured with an Aviv model 202 CD spectrometer (Aviv Instruments, Lakewood, CO, USA). Temperature regulation was carried out with the built-in temperature control device. Thermal unfolding and denaturation of the hemoglobins was studied between 25 and 60°C. Buffered hemoglobin solutions (preparation see above) with c = 0.1 mg/ml were prepared. The hemoglobin solutions were first adjusted to 25°C and then the temperature increased stepwise (equilibration time: 1 min). Afterwards, a complete wavelength scan (wavelength steps: 1 nm, average time: 4 s) was carried out in the far UV-region between 190 and 260 nm. Blank spectra of buffer solutions were subtracted from the Hb spectra at each temperature point and the offset was corrected at 250 nm. Absolute ellipticity at 222 nm was assumed, representing a measure of the alpha-helical content of the protein (Greenfield 1996) and plotted against temperature.

Protein amino acid sequences and computational analysis

Protein amino acid sequences were obtained from NCBI PubMed online database (www.ncbi.com). Multiple sequence alignments were performed under usage of the ClustalX (1.83) software (Higgins et al. 1991) and visualized with Microsoft Office standard software. Molecular weights were predicted under usage of the analysis tools on the ExPASy Server according to Gasteiger et al. (2005). Predicted secondary structure compositions (α-helical contents) were calculated online according to Corpet et al. (1998) under usage of available protein amino acid sequences from NCBI PubMed online database.

Results

Diffusion coefficients and hydrodynamic radii of hemoglobin molecules were measured with DLS at a temperature range between 21 and 51°C. Either continuous temperature scans (scan rate: 0.1–0.2°C/min) or a stepwise increase of temperature (5–10 min per step, heating rate: 1°C/min) was performed. Figure 2 shows a representative DLS graph for hemoglobins of *T. aculeatus* (T_B: 33.0°C), *Homo sapiens sapiens* (T_B: 36.6°C) and *Bos taurus taurus* (T_B: 38.6°C). The R_H was plotted against the temperature. The used Astra 5.1 software of the DLS device gave the R_H directly calculated from the auto correlation function as an average over the whole particles in the observed volume. In DLS experiments, the R_H of hemoglobin molecules increased linearly with temperature. At the critical transition temperature, T_C, the slope of the curves suddenly rose (Fig. 2). The coefficient of diffusion correlates inversely with the hydrodynamic radius (Einstein–Stokes equation, Eq. 1).

In Table 1, the average hydrodynamic radii (R_H at 25°C), the calculated coefficients of diffusion (D at 25°C), the animals' body temperatures (T_B) and the structural transition temperatures (T_C) of six different hemoglobins are shown. The R_H and D of the examined hemoglobins were similar for *Homo sapiens sapiens*, *Bos taurus taurus*, and *O. anatinus* hemoglobins. The hydrodynamic radii for *Homo sapiens sapiens* (3.59 nm) and *Bos taurus taurus* hemoglobins (3.83 nm) were in good agreement with published data (Arosio et al. 2002). *Gallus gallus domesticus* hemoglobin showed a larger radius at 4.43 nm. *Sus scrofa domestica* hemoglobin and *T. aculeatus* hemoglobin had very large R_H's with 12.70 and 8.82 nm, respectively. In order to interpret the DLS data meaningfully it is important to know what the distributions of sizes are within the sample. These results indicate a strong formation of hemoglobin aggregates even in diluted solutions at 25°C.

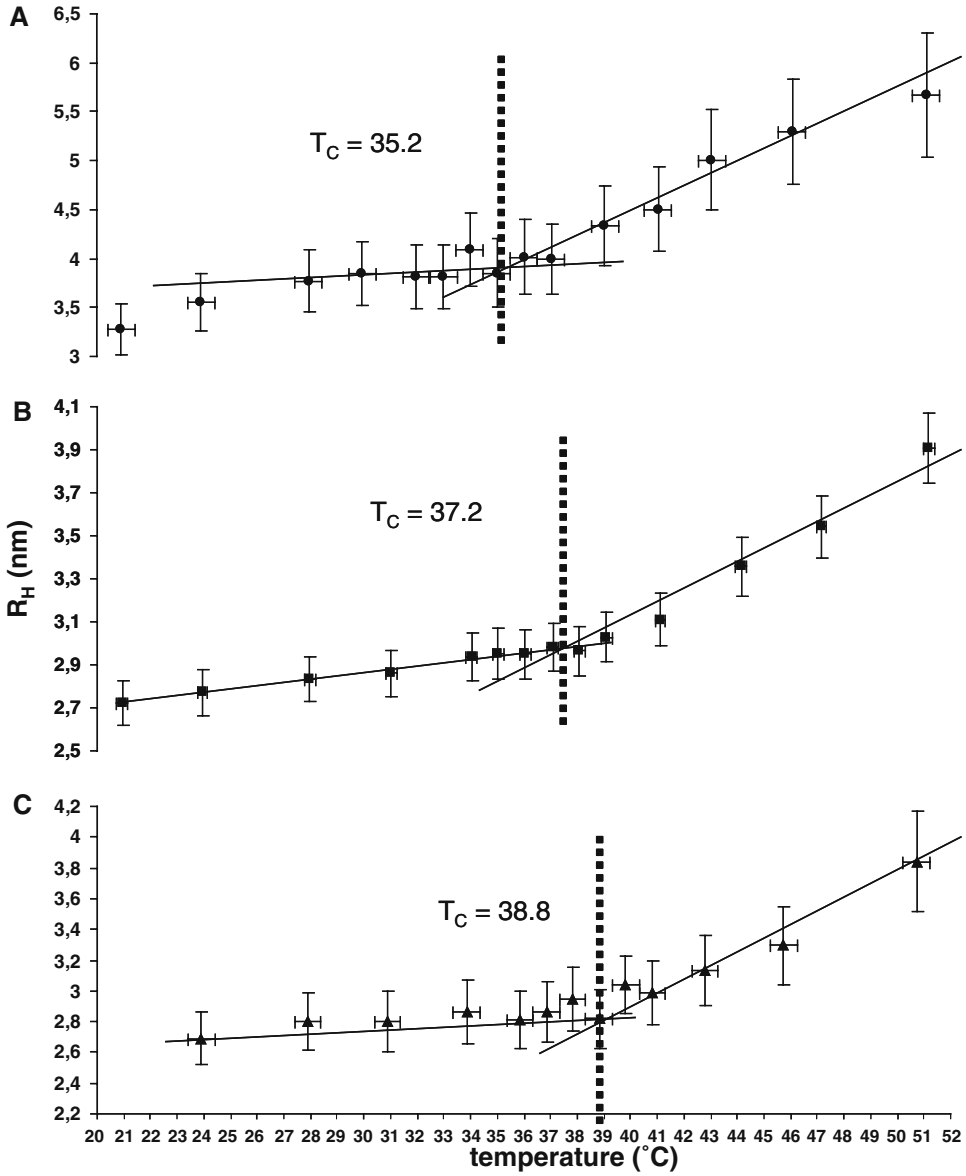

Fig. 2 Typical graph of DLS data from hemoglobin of *Ornithorhynchus anatinus* (**a** T_B = 33.0 ± 1.0), *Homo sapiens sapiens* (**b** T_B = 36.6 ± 0.2), and *Bos taurus taurus* (**c** T_B = 38.6 ± 0.3). The hydrodynamic radii (R_H) are plotted against temperature. For the individual presented measurements the obtained structural transition temperatures (T_C) are given

Table 1 Dynamic light scattering data showing the species' name, respective body and transition temperatures as well as the averaged hydrodynamic radii (R_H) and the coefficients of diffusion (D) at 25°C

Light scattering data (DLS)				
Species	Body-temperature (°C)	Structural transition-temperature (°C)	R_H 25°C (nm)	D 25°C (m^2/sec) × 10^{-11}
Tachyglossus aculeatus	33.0 ± 1.0	34.9 ± 1.3	8.82 ± 0.23	2.76 ± 0.01
Ornithorhynchus anatinus	33.0 ± 1.0	33.4 ± 2.1	3.49 ± 0.25	6.98 ± 0.02
Homo sapiens sapiens	36.6 ± 0.2	36.4 ± 0.8	3.59 ± 0.09	6.79 ± 0.02
Bos taurus taurus	38.6 ± 0.3	38.1 ± 1.9	3.83 ± 0.16	6.36 ± 0.02
Sus scrofa domesticus	39.7 ± 0.5	40.1 ± 1.3	12.70 ± 4.38	1.92 ± 0.01
Gallus gallus domesticus	41.0 ± 0.5	41.8 ± 1.9	4.43 ± 0.28	5.50 ± 0.02

All samples were derived from fresh blood except for *Sus scrofa domesticus*, in this exceptional case, purchased crystallized hemoglobin powder was used. Initial (at 25°C) differences in R_H for different samples indicate some level of incipient Hb aggregation, which corresponds to some extent to the situation in blood

Nevertheless, in all studied hemoglobin samples an increase of the R_H was visible independent of the starting R_H at 25°C. Multiple repeats, lengthy temperature scans and extensive statistical analysis were applied in order to overcome initial polydispersity of the samples and to increase feasibility and reliability of the data. As described at a critical transition temperature, T_C, the slope of the curves suddenly rose. This means a more accelerated increase of R_H above T_C and can be interpreted as an increased amount of aggregated particles and most likely not as a slight modification of the hydrodynamic shapes due to partial unfolding. Further details of this effect may be studied using size exclusion chromatography combined with static light scattering. This would be one way to avoid for example small contamination in the sample.

In CD experiments, the temperature dependency of the ellipticity at 222 nm was observed. Data plots of three typical CD experiments with hemoglobin from *C. wagneri* (Fig. 3a $T_B = 36.17 \pm 0.5$), *C. bactrianus* (Fig. 3b $T_B = 38.0 \pm 0.5$), and *E. helias* (Fig. 3c $T_B = 41.06 \pm 0.5$) are shown in Fig. 3. In total, hemoglobins from 11 different species were studied with CD experiments. At 222 nm, CD spectra are most sensitive to changes in the α-helical content of proteins. When plotting the ellipticity (in mdeg) versus temperature, in all species two transition points appeared and the curves were s-shaped (with increasing

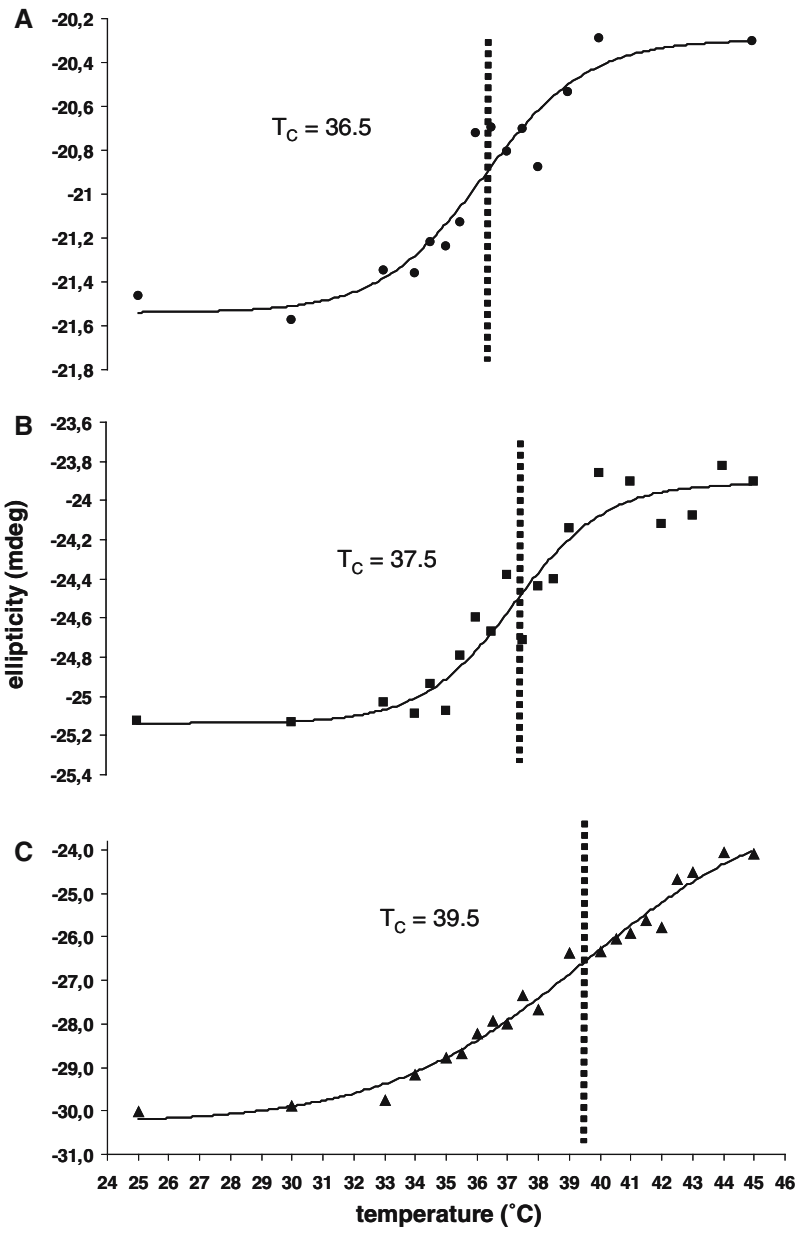

Fig. 3 Original plot of three typical circular dichroism experiments with hemoglobin from *Catagonus wagneri* (**a** $T_B = 36.17 \pm 0.5$), *Camelus bactrianus* (**b** $T_B = 38.0 \pm 0.5$), and *Eurypyga helias* (**c** $T_B = 41.06 \pm 0.5$). The ellipticities are plotted against temperature. The midpoint temperatures of the fitted *sigmoid curves* were defined as structural transition temperature (see also Digel et al. 2006; Artmann et al. 2004). For the individual presented measurements the obtained structural transition temperatures (T_C) are given

temperature: low slope, high slope, low slope). The critical temperature, T_C, was taken to be the midpoint temperature between the low- and the high-change point was taken (Fig. 3) to obtain the structural transition temperature. The results of this analysis are presented in Table 2.

Circular dichroism and DLS experiments carried out in parallel with identical hemoglobin samples (*T. aculeatus*, *O. anatinus*, *Homo sapiens sapiens*) showed that the T_C obtained with DLS and T_C from CD measurements were the same within experimental errors (see also Digel et al. 2006). However, due to the lack of the concurrent availability of DLS-, CD instruments and blood samples, it was impossible to study all selected blood samples using both of these methods. The structural transition temperatures obtained with either type of experiments on hemoglobins from a total of 14 different species were plotted against body temperatures (Fig. 4). The temperature transitions occurred in all hemoglobins from selected species. They correlated linearly with the species' body temperature (slope 0.81, $r = 0.95$).

The studied hemoglobins show very similar molecular properties, e.g., molecular weight, amino acid chain length

Table 2 Table of circular dichroism results showing species' name, respective body and transition temperatures

Circular dichroism data		
Species	Body-temperature (°C)	Structural transition-temperature (°C)
Tachyglossus aculeatus	33.0 ± 1.0	34.0 ± 0.5
Ornithorhynchus anatinus	33.0 ± 1.0	34.0 ± 0.5
Phascolarctos cinereus	35.2 ± 0.5	36.5 ± 1.5
Catagonus wagneri	36.17 ± 0.5	36.5 ± 0.5
Homo sapiens sapiens	36.6 ± 0.2	37.1 ± 0.5
Thylogale sp.	37.0 ± 0.5	36.7 ± 0.5
Felis viverrina	37.6 ± 0.5	37.3 ± 1.0
Felis silvestris forma catus	37.7 ± 0.5	37.0 ± 1.0
Camelus bactrianus	38.0 ± 0.5	37.5 ± 0.5
Eurypyga helias	41.06 ± 0.5	39.5 ± 1.0
Nucifraga caryocatactes	42.2 ± 0.5	42.0 ± 1.0

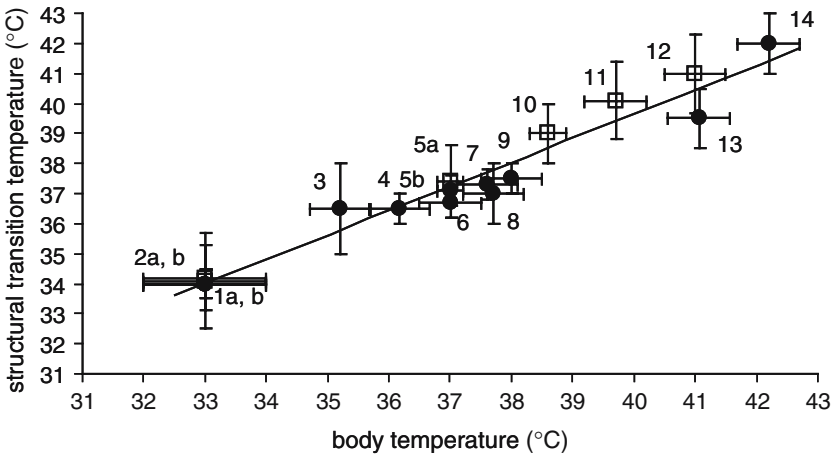

Fig. 4 Correlation between structural transition temperatures of hemoglobins from various species (including *Homo sapiens sapiens*) and the species' body temperature. Circular dichroism data are shown as *black circles*; dynamic light scattering data are drawn as *open squares*. The *line* represents a linear regression fit with a slope of 0.81 and a coefficient of correlation of 0.97. *Numbers* at the data points represent individual species: 1a and 1b *Ornithorhynchus anatinus* (platypus), 2a and 2b *Tachyglossus aculeatus* (echidna), 3. *Phascolarctos cinereus* (coala), 4. *Catagonus wagneri* (chacoan peccary), 5a and 5b *Homo sapiens sapiens* (human), 6. *Thylogale* sp. (dusty pademelon), 7. *Felis viverrina* (fishing cat), 8. *Felis silvestris* forma *catus* (felis serval), 9. *Camelus bactrianus* (bactrian camel humphrey), 10. *Bos taurus taurus* (cow), 11. *Sus scrofa domestica* (pig), 12. *Gallus gallus domesticus* (chicken), 13. *Eurypyga helias* (greater sunnbittern), and 14. *Nucrifraga caryocatactes* (spotted nutcracker)

Table 3 Known parameters of the studied hemoglobins of various species

Species	Molecular weight (kDa)	Number of amino acids per subunit		α-helical content (%)
		α	β	
Tachyglossus aculeatus[a]	63.14 or 63.58	141, 141	147	77.8
Ornithorhynchus anatinus	62.4	141	146	78.1
Homo sapiens sapiens	62.52	142	147	76.5
Felis silvestris forma catus	62.48	141	146	77.4
Camelus bactrianus	62.84	141	147	78.2
Bos taurus taurus	62.26	142	145	78.1
Sus scrofa domesticus	62.42	141	147	77.1
Gallus gallus domesticus[a]	63.80 or 64.32	142, 141	147	76.9, 77.5

All values were calculated using online predictions: the data for predicted secondary structure composition for the proteins was calculated online according to Corpet et al. (1998). Molecular weights were calculated under usage of ExPAsy ProtParam tool according to Gassteiger et al. (2005). All predictions based on NCBI database protein sequences (http://www.ncbi.nlm.nih.gov/entrez/)

[a] For *Tachyglossus aculeatus* and *Gallus gallus domesticus* two different α-subunits do exist (A1, A2 and Aa, Ad, respectively), this was considered in all calculations

of the subunits and α-helical content (Table 3). All amino acid sequences of the studied hemoglobins (α- and β-subunits) available in online databases were aligned under usage of ClustalX (1.83) software. Results were presented in Fig. 5 (Fig. 5a α-subunits, Fig. 5b β-subunits). The predicted α-helical parts of the subunits were marked gray. Total averaged similarity of the amino acid parts was calculated. In both subunits the first two α-helical parts of the sequences (amino acid numbers 7–32) were interestingly of low similarity. Both parts are located at external parts of the subunit (solvent exposed). In contrast to this the other parts of the subunits, especially the middle parts (which were located in the inside 3D structure of the protein with contacts to the heme group) show high similarities of 70–100%.

Discussion

It was proposed that the effect of rapid RBC passage changes observed in micropipette aspiration experiments at T_C (Artmann et al. 1998) could be attributed to a high-to-low hemoglobin viscosity transition mediated by a partial release of hemoglobin-bound water. Subsequent to the unfolding of the α-helices molecular hemoglobin aggregation might be observed (Kelemen et al. 2001). Based on two-dimensional infrared spectroscopy, a two-step model of protein unfolding in human hemoglobin was considered (Yan et al. 2004, 2003). First, an initial structural perturbation between 30 and 44°C and second, thermal protein unfolding within the temperature range of 44–54°C followed by the unfolding of solvent exposed helical structures. The second step is irreversible and induces thermal aggregation between 54 and 70°C due to the exposure of formerly buried hemoglobin chains (Fig. 2). Similar results were obtained for myoglobin and ribonuclease (Yan et al. 2002, 2003, 2004). None of these studies mentioned a particular transition at body temperature.

To summarize, structural changes of hemoglobin determine some biophysical effects visible in single cell micropipette and viscometry experiments on a macroscopic scale. Studies of Artmann et al. (2004), Digel et al. (2006) and this study attempted to observe a temperature-dependent molecular effect of hemoglobin. It was possible to detect a structural transition of hemoglobin at T_B using CD spectroscopy that was first described in 2004 (Artmann et al. 2004). In these experiments, the loss of α-helical content in human hemoglobin underwent an accelerated ellipticity loss at around 36.4°C. It was assumed that this effect plays a singular role in the initial structural perturbation stage model (Yan et al. 2003). Further comparative CD and DLS studies (Digel et al. 2006) using blood samples taken from primitive mammalians revealed Hb transition for monotremes at their body temperature. The authors speculated that the structural transition point of mammalians' Hb is related to species' physiological core body temperature that might, in turn, have general biological relevance in respect of body temperature sensing and management. This correlation was proofed and presented in the results of this study. From a physiological point of view, one might speculate that the drop in hemoglobin solution viscosity observed near to the body temperature (Kelemen et al. 2001) occurs inside whole RBCs as well when passing the peripheral vasculature where there are many small vessels and significantly lower temperatures. This might well be the case in particular in microcirculatory situations where many RBCs within a short time have to pass narrow obstacles as for example in

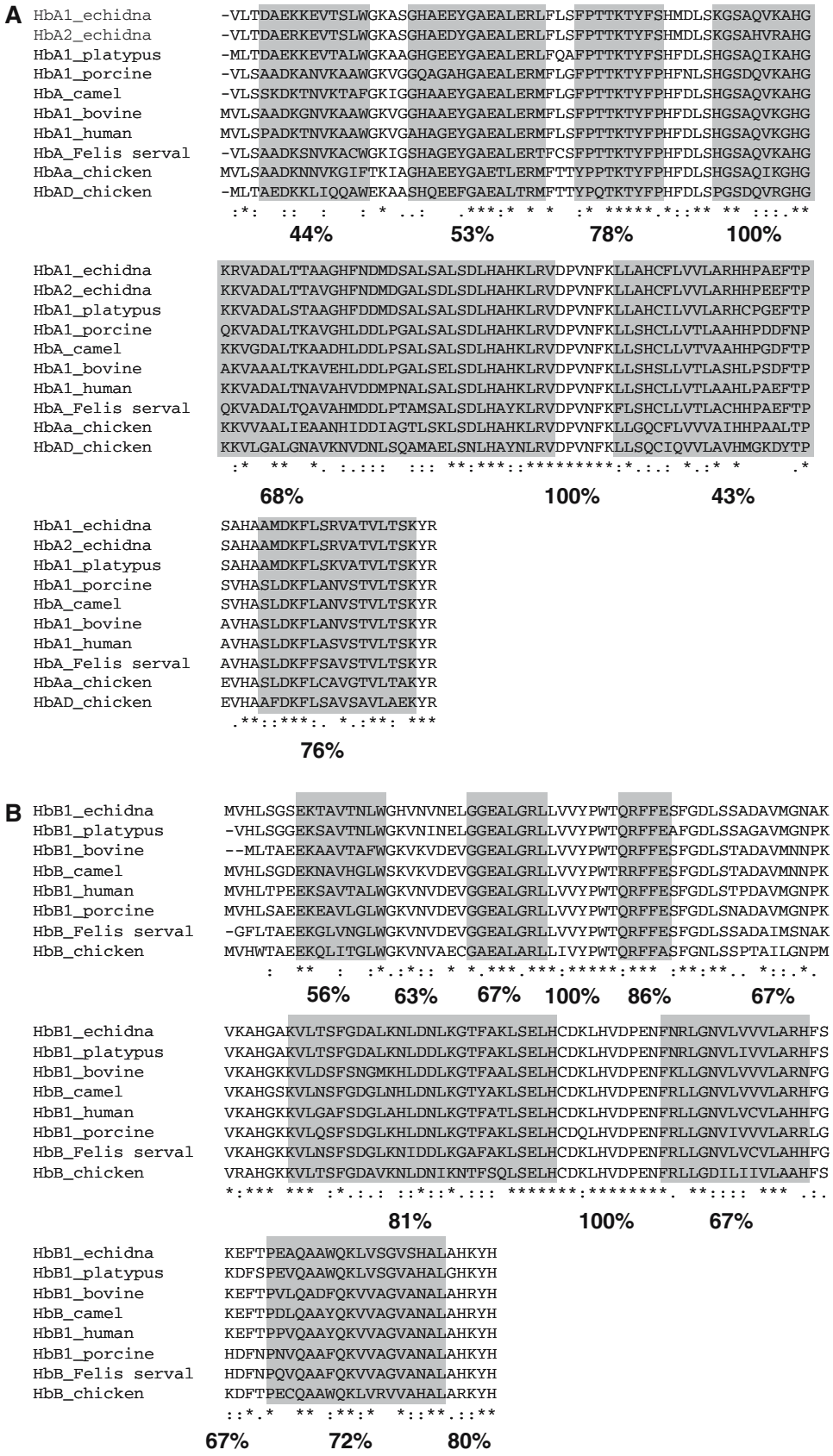

Fig. 5 Amino acid sequence alignment of hemoglobin subunits α and β of all species whose sequences were available online (NCBI database). **a** Hemoglobin α-subunits, **b** hemoglobin β-subunits. The *gray* background indicates predicted α-helical contents of the subunits. For each section an amino acid sequence similarity between all hemoglobins is given (*asterisk* identical amino acids, *colon* similar amino acids, *dot* less similar amino acids)

the eyes microvasculature (Hecking et al. 2006). About the molecular mechanisms of the structural transitions observed at T_C, more information needs to be obtained. It could prove helpful to use specific methods for structural studies on proteins, such as nuclear magnetic resonance spectroscopy or neutron scattering, among others. A possible method to study high-concentrated protein solutions is neutron scattering. First neutron scattering experiments on the dynamical transition in a protein were elastic scans on myoglobin powders hydrated with D_2O (Biscout and Zaccai 2001; Doster et al. 1989). Methods have been developed to study hemoglobin in intact RBCs (Krueger and Nossal 1988; Garvey et al. 2004) and in concentrated hemoglobin solutions (Krueger et al. 1990). Under usage of neutron scattering a scanning of a temperature range about body temperature might be done. Neutron scattering might make it possible to show the structural transition in intact and unsheared RBCs. So it may be a good method to study hemoglobin in its natural environment.

The probably conformational changes observed in this study represent more subtle potential minima in conformation of the protein. For this reason, the usage of small angle scattering (Garvey et al.2004; Krueger et al. 1990; Krueger and Nassal 1988), pulsed field gradient NMR (Kuchel and Chapman 1991) and quasi-elastic neutron scattering (Longeville et al. 2003) may be more appropriate experimental tools to link conformational changes in the Hb tetramer to changes in the bulk viscosity of the intracellular solution.

It appears possible to detect at which site of the protein an accelerated unfolding of α-helices begin when the experimental temperature approaches body temperature. The question to address now is whether there exists a particular structural motif hidden in the hemoglobin molecule determining the transition. Finally, it is important to check if there is a motif, which changes would determine the tiny differences in the transition temperatures between hemoglobins of different species.

A first consideration can be made based on the amino acid sequence alignments (Fig. 5). In the α- and β-subunits of hemoglobin the first two α-helical parts of the sequences (amino acid numbers 7–32) were of low similarity. Both parts are located at external parts of the subunit (solvent exposed) what can be seen in 3D pictures of human hemoglobin (Park et al. 2006). In contrast to the heme-connected inner protein parts which are very conserved (amino acid numbers 50–100, sequence similarity up to 100%) both first α-helical parts of hemoglobin's α- and β-subunits (amino acid numbers 7–32) are of low similarity. If it can be hypothesized that information about a T_B-specific behavior of hemoglobins can be imprinted in the protein structure. A sequence part with low conserved sequence similarity but highly conserved structural elements (α-helix) might be very promising for further studies. In other words, nature may know by protein structure where body temperature has to be set on the temperature scale. Contrariwise it can be speculated if the hemoglobin structure is an evolutionary consequence of the species' specific variable body temperature.

These findings and their implications might initiate new research in cell biology and biophysics with special emphasis on non-linear effects occurring around T_B. On a molecular level, it might be possible in the future to understand why body temperature is so particular to a species and which structural motif dominates in determining this. Finally, as preliminary studies suggest, important similar transitions also occur at body temperature in other proteins with very different functions in our body.

Acknowledgments This work was financed by a grant from the Ministry of Innovation, Science, Research and Technology of the State of North Rhine-Westphalia to G. M. Artmann and by the Centre of Competence in Bioengineering at Juelich, Germany. We thank Jeff Turnage, San Diego Zoological Society, San Diego, CA, USA, for supplying animal blood samples. We thank Prof. Shu Chien and Prof. Y. C. Fung, Whittaker Institute for Bioengineering (UCSD), San Diego, for interesting and helpful discussions. Finally, we thank our colleagues Prof. G. Büldt and PD Dr. Fitter, Research Centre Juelich, for their support in structural biology. We also thank Prof. G. Dikta, who gave us excellent advice on statistical methods for turning point determinations.

References

Arosio D, Kwansa HE, Gering H, Piszczek G, Bucci E (2002) Static and dynamic light scattering approach to the hydration of hemoglobin and its supertetramers in the presence of osmolites. Biopolymers 63:1–11

Artmann GM, Burns L, Canaces JM, Temiz Artmann A, Schmid-Schönbein GW, Chien S, Maggakis-Kelemen C (2004) Circular dichroism spectra of human hemoglobin reveal a reversible structural transition at body temperature. Eur Biophys J 33:490–496

Artmann GM, Kelemen C, Porst D, Büldt G, Chien S (1998) Temperature transitions of protein properties in human red blood cells. Biophys J 75:3179–3183

Berne BJ, Pecora R (1976) Dynamic light scattering. Wiley, New York

Biscout DJ, Zaccai G (2001) Protein flexibility from the dynamical transition: a force constant analysis. Biophys J 80:1115–1123

Cameron IL, Ord VA, Fullerton GD (1988) Water of hydration in the intra- and extra-cellular environment of human erythrocytes. Biochem Cell Biol 66:1186–1199

Corpet F, Gouzy J, Kahn D (1998) The ProDom database of protein domain families. Nucleic Acids Res 26:323–326

Digel I, Maggakis-Kelemen C, Zerlin KF, Linder P, Kasischke N, Kayser P, Porst D, Temiz Artmann A, Artmann GM (2006) Body temperature-related structural transition of monotremal and human hemoglobin. Biophys J 91:1–8

Doster W, Cusack S, Petry W (1989) Dynamical transition of myoglobin revealed by inelastic neutron scattering. Nature 337:754–756

Garvey CJ, Knott RB, Drabarek E, Kuchel PW (2004) Shear-induced alignment of self-associated hemoglobin in human erythrocytes: small angle neutron scattering studies. Eur Biophys J 33:589–595

Gasteiger E, Hoogland C, Gattiker A, Duvaud S, Wilkins MR, Appel RD, Bairoch A (2005) Protein identification and analysis tools on the ExPASy Server. In: Walker JM (ed) The proteomics protocols handbook. Humana Press, Totowa, pp 571–607

Glaser R (2004) Biophysics. Springer, Berlin

Greenfield NJ (1996) Methods to estimate the confirmation of proteins and polypeptides from circular dichroism data. Anal Biochem 235:1–10

Grigg GC, Beard LA, Barnes JA, Perry LI, Fry GJ, Hawkins M (2003) Body temperature in captive long-beaked echidnas (Zoglossus Bartoni). Comp Biochem Physiol A Mol Integr Physiol 136:911–916

Hecking C, Aschwanden M, Dickenmann M, Thalhammer C, Blum B, Bilecen D, Jaeger KA (2006) Efficient haemodialysis despite complete central venous thrombosis. Vasa 35:243–244

Higgins DG, Bleasby AJ, Fuchs R (1991) Clustal V: improved software for multiple sequence alignment. Comput Appl Biosci 8:189–191

Kelemen C, Chien S, Artmann GM (2001) Temperature transition of human hemoglobin at body temperature: effects of calcium. Biophys J 80:2622–2630

Krueger S, Chen S-H, Hofrichter J, Nossal R (1990) Small angle neutron scattering studies of HbA in concentrated solutions. Biophys J 58:745–757

Krueger S, Nossal R (1988) SANS studies of interacting hemoglobin in intact erythrocytes. Biophys J 53:97–105

Kuchel PW, Chapman BE (1991) Translational diffusion of hemoglobin in human erythrocytes and hemolysates. J Magn Reson 95:574–580

Longeville S, Doster W, Kali G (2003) Myoglobin in crowded solutions: structure and diffusion. Chem Phys 292:413–424

Park SY, Yokoyama T, Shibayama N, Shiro Y, Tame JR (2006) 1.25 A resolution crystal structures of human haemoglobin in the oxy, deoxy and carbonmonoxy forms. J Mol Biol 360:690–701

Penzlin H (1977) Lehrbuch der tierphysiologie. Gustav Fischer Verlag, Stuttgart, New York

Van Kampen EJ, Zijlstra WG (1965) Determination of hemoglobin and its derivatives. Advances in clinical chemistry. Sobotka and Steward, vol 8. Academic, New York, London

Whittow C (1971) Comparative physiology of thermoregulation, vol 2. Mammals Academic, New York, London

Yan Y-B, Wang Q, He H-W, Zhou H-M (2004) Protein thermal aggregation involves distinct regions: sequential events in the heat-induced unfolding and aggregation of hemoglobin. Biophys J 86:1682–1690

Yan Y-B, Wang Q, He H-W, Hu X-Y, Zhang R-Q, Zou H-M (2003) Two-dimensional infrared correlation spectroscopy study of sequential events in the heat-induced unfolding and aggregation process of myoglobin. Biophys J 85:1959–1967

Yan Y-B, Zhang R-Q, Zhou H-M (2002) Biphasic reductive unfolding of ribonuclease A is temperature dependent. Eur J Biochem 269:5314–5322

Zwart A, Buursma A, van Kampen EJ, Zijlstra WG (1984) Multicomponent analysis of hemoglobin derivatives with a reversed-optics spectrophotometer. Clin Chem 30:373–379